HAL
open science

Reactions of lithium salts of triphosphines tBu2P–PLi–PtBu2 and tBu2P–PLi–P(NEt2)2 with metal complexes [(R3P)2MCl2] (M = Ni, Pd, Pt, R3P = Et3P, pTol3P, Ph2EtP, iPr3P)

Aleksandra Wiśniewska, Katarzyna Baranowska, Rafal Grubba, Eberhard Matern, Jerzy Pikies

To cite this version:

Aleksandra Wiśniewska, Katarzyna Baranowska, Rafal Grubba, Eberhard Matern, Jerzy Pikies. Reactions of lithium salts of triphosphines tBu2P–PLi–PtBu2 and tBu2P–PLi–P(NEt2)2 with metal complexes [(R3P)2MCl2] (M = Ni, Pd, Pt, R3P = Et3P, pTol3P, Ph2EtP, iPr3P). Journal of Inorganic and General Chemistry / Zeitschrift für anorganische und allgemeine Chemie, 2010, 636 (8), pp.1549. 10.1002/zaac.200900540 . hal-00552435

HAL Id: hal-00552435

https://hal.science/hal-00552435v1

Submitted on 6 Jan 2011

HAL is a multi-disciplinary open access archive for the deposit and dissemination of scientific research documents, whether they are published or not. The documents may come from teaching and research institutions in France or abroad, or from public or private research centers.

L'archive ouverte pluridisciplinaire **HAL**, est destinée au dépôt et à la diffusion de documents scientifiques de niveau recherche, publiés ou non, émanant des établissements d'enseignement et de recherche français ou étrangers, des laboratoires publics ou privés.

Zeitschrift für Anorganische und Allgemeine Chemie

Reactions of lithium salts of triphosphines tBu2P–PLi–PtBu2 and tBu2P–PLi–P(NEt2)2 with metal complexes [(R3P)2MCl2] (M = Ni, Pd, Pt, R3P = Et3P, pTol3P, Ph2EtP, iPr3P)

Journal:	*Zeitschrift für Anorganische und Allgemeine Chemie*
Manuscript ID:	zaac.200900540.R1
Wiley - Manuscript type:	Article
Date Submitted by the Author:	10-Feb-2010
Complete List of Authors:	Wiśniewska, Aleksandra; Gdańsk University of Technology, Faculty of Chemistry Baranowska, Katarzyna; Gdańsk University of Technology, Faculty of Chemistry Grubba, Rafał; Gdańsk University of Technology, Faculty of Chemistry Matern, Eberhard; Institut für Anorganische Chemie, Universität Karlsruhe (TH) Pikies, Jerzy; Gdańsk University of Technology, Faculty of Chemistry
Keywords:	P ligands, platinum, nickel, palladium

scholarONE Manuscript Central

Reactions of lithium salts of triphosphines $^{t}Bu_2P–PLi–P^{t}Bu_2$ and $^{t}Bu_2P–PLi–P(NEt_2)_2$ with metal complexes $[(R_3P)_2MCl_2]$ (M = Ni, Pd, Pt, R_3P = Et_3P, $^{p}Tol_3P$, Ph_2EtP, $^{i}Pr_3P$)

Aleksandra Wiśniewska[a], Katarzyna Baranowska[a], Rafał Grubba[a], Eberhard Matern[b], Jerzy Pikies[a*].

[a] Faculty of Chemistry, Department of Inorganic Chemistry, Gdańsk University of Technology, G. Narutowicza St. 11/12. PL-80-233 Gdańsk, Poland

[b] Institut für Anorganische Chemie, Universität Karlsruhe (TH), Engesserstraße 15, D-76128 Karlsruhe, Germany

Received

[*] Prof. Dr. Jerzy Pikies

Faculty of Chemistry,

Department of Inorganic Chemistry,

Gdańsk University of Technology,

G. Narutowicza St. 11/12, PL-80-233 Gdańsk, Poland

e-mail: jerzy.pikies@pg.gda.pl

Abstract. $^{t}Bu_2P–PLi–P^{t}Bu_2·2THF$ reacts with $[(R_3P)_2MCl_2]$ (M = Pt, Pd, Ni) yielding isomers of $[(1,2-\eta-^{t}Bu_2P=P–P^{t}Bu_2)M(PR_3)Cl]$ where $^{t}Bu_2P–P–P^{t}Bu_2$ ligand adopts the geometry of a side-on bonded 1,1-di-*tert*-butyl-2-(di-*tert*-butylphosphino)diphosphenium cation. $^{t}Bu_2P–PLi–P(NEt_2)_2·2THF$ reacts with $[(R_3P)_2MCl_2]$ but does not formed complexes with a $^{t}Bu_2P–P–P(NEt_2)_2$ moiety, however, splitting of a $P–P(NEt_2)_2$ bond of the parent triphosphine takes place.

Keywords: P ligands; nickel, palladium, platinum.

1. Introduction

Phosphido and phosphinidene complexes of transitions metals are versatile reagents in syntheses of phosphorus – element bond [1].

The reactivity of metal phosphides and silylphosphides towards complexes of nickel triad was studied for three decades. $LiP(SiMe_3)_2$ reacts with $[Cp(Cl)Ni(PPh_3)]$ at low temperature yielding unstable terminal phosphido complex [2], similarly $[(R_3P)_2NiCl_2]$ reacts with $LiP(SiMe_3)_2$ at low temperature yielding unstable mono and diphosphido NI(II) complexes which decompose under formation of cyclic Ni(I) complexes $[R_3P\text{-}Ni\{\mu\text{-}P(SiMe_3)_2\}]_2$*(Ni-Ni)* and side-on bonded diphosphene complexes $[(R_3P)_2Ni(\eta^2\text{-}Me_3SiP{=}PSiMe_3)]$ [3,4,5,6]. Similar behaviour was observed in reactions of $[(dRpe)NiCl_2]$ with $LiP(SiMe_3)_2$ (dRpe = $R_2PCH_2CH_2PR_2$), the diphosphorous complexes $[(R_3P)_2Ni(\mu\text{-}P_2)Ni(PR_3)_2]$ were thereafter isolated.[7,8]. The reactions of LiP^tBu_2 with $[(Me_3P)_2NiCl_2]$ yielded $[Me_3P\text{-}Ni\{\mu\text{-}P^tBu_2\}]_2$*(Ni-Ni)* [9]. Thus, the phosphido ligands tend to occupy bridge positions while the stable Ni-complexes with terminal phosphido groups are rare. Driess *et al.* reported on the synthesis and X-ray structure of $[Cp(Ph_3P)NiPH(SiFTrip_2)]$ [10] and Hilhouse *et al*. reported on complex $[(dtbpe)NiP^tBu_2]$ [11] (dtbpe = $^tBu_2PCH_2CH_2P^tBu_2$). In both cases the geometry around phosphido P atoms is pyramidal.

The data on palladium phosphido-complexes are scarce. Reduction of [*cis*-$(Cy_2HP)_2PdCl_2$] with sodium yields phosphido bridged Pd(I) complex $[Cy_2HPPd\{\mu\text{-}PCy_2\}]_2$*(Pd-Pd)* [12]. $[(Et_3P)_2PdCl_2]$ reacts with $^tBu_2P{-}P{=}P^tBu_2(Me)$ in the presence Na/Nph yielding $[Et_3PPd\{\mu\text{-}P^tBu_2\}]_2$*(Pd-Pd)* [13]. Terminal phosphido Pd(II) complexes were isolated only for cyclic compounds $[(diphos)Pd\{(CH_2C_6H_2Me_2)Pd(Mes)\}]$ [14].

$LiP(SiMe_3)_2$ reacts with $[(R_3P)_2PtCl_2]$ yielding initially unstable terminal mono and diphosphido Pt(II) complexes. These complexes decompose at r. t. giving rise to Pt(I) complexes $[Et_3P\text{-}Pt\{\mu\text{-}P(SiMe_3)_2\}]_2$*(Pt-Pt),* side-on bonded diphosphene complexes $[(Et_3P)_2Pt(\eta^2\text{-}Me_3SiP{=}PSiMe_3)]$ and diphosphorous complexes $[(R_3P)_2Pt(\mu\text{-}P_2)Pt(PR_3)_2]$ [15]. The terminal phosphido complexes of Pt (II) are more stable than related complexes of Ni and Pd. [*cis*-$(PHCy_2)PtCl_2$] reacts with sodium at

r. t. yielding $[Cy_2HPPt\{\mu\text{-}PCy_2\}]_2$*(Pt-Pt)* and a stable complex [*trans*-$(Cy_2HP)_2PtCl(PCy_2)$]. The geometry around terminal phosphido P-atom is pyramidal [16]. A series of stable terminal Pt (II) phosphido complexes [(dppe)Pt(Me)X] (X = PHR or PR_2) was described [17]. For the latest review see [18].

We have studied the reactivity of litiated diphosphines $R'_2P–P(SiMe_3)Li$ and lithiated triphosphine $^tBu_2P–PLi–P^tBu_2$ towards transition metals complexes. The reaction of $[(R_3P)_2PtCl_2]$ with $R'_2P–P(SiMe_3)_2$ involves mainly a formation of dinuclear diphosphorous complexes $[(R_3P)_2Pt(\mu\text{-}P_2)Pt(PR_3)_2]$ [19], and, with $R'_2P–P(SiMe_3)Li$ the formation of side-on bonded phosphanylphosphinidene complexes $[(\eta^2\text{-}R'_2P{=}P)Pt(PR_3)_2]$ but not phosphido complexes. This reaction is relatively general, R' can adopt ^tBu, ^iPr, Et_2N and $^iPr_2N$, but not Ph [20].

$^tBu_2P–PLi–P^tBu_2{\cdot}2THF$ reacts with $[(Et_3P)_2MCl_2]$ (M = Ni, Pd) yielding mixtures of isomers of $[(1,2\text{-}\eta\text{-}^tBu_2P{=}P–P^tBu_2)M(PEt_3)Cl]$. The related reaction with [*cis*-$(Et_3P)_2PtCl_2$] does not yield $[(1,2\text{-}\eta\text{-}^tBu_2P{=}P–P^tBu_2)Pt(PEt_3)Cl]$ [21]. Homologous $[(1,2\text{-}\eta\text{-}^tBu_2P{=}P–P^tBu_2)Pt(PPh_3)Br]$ was obtained in a different way and proved to be quite stable [22]. According to the structural and ^{31}P-NMR data these complexes can be viewed as a modification of side-on bonded phosphanyl-phosphinidene complexes rather, than as terminal phosphido complexes [20].

Now we have extended our investigations on the reactivity of $^tBu_2P\text{-}PLi\text{-}P^tBu_2{\cdot}2THF$ with $[(R_3P)_2MCl_2]$ (M = Ni, Pd, Pt) where R groups possess different electronic and steric properties. Moreover, we have studied the reactivity of $^tBu_2P–PLi–P(NEt_2)_2{\cdot}2THF$ towards $[(R_3P)_2MCl_2]$ (M = Ni, Pd, Pt)

2. Results and Discussion

2.1. Reactivity

The reaction of $[(R_3P)_2MCl_2]$ (M = Pd, Ni) with 1 molar equiv. of $^tBu_2P–PLi–P^tBu_2{\cdot}2THF$ in THF at room temperature yields two isomers of $[(1,2\text{-}\eta\text{-}^tBu_2P{=}P–P^tBu_2)M(PR_3)Cl]$ (**a** and **b**) (Scheme 1).

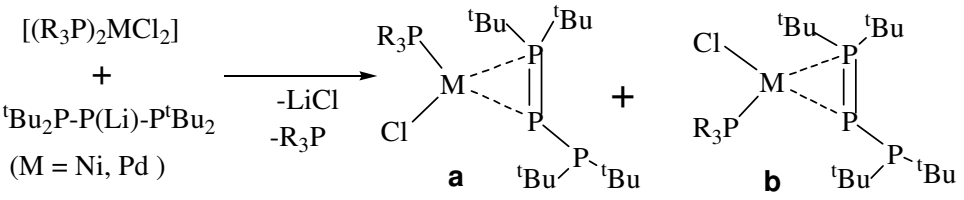

Scheme 1

However this reaction with platinum complex $[(^{p}Tol_3P)_2PtCl_2]$ gave only one isomer **a**. We have isolated $[(1,2\text{-}\eta\text{-}^{t}Bu_2P{=}P{-}P^{t}Bu_2)Pt(^{p}Tol_3P)Cl{\cdot}C_5H_{12}]$ (**1a·pentane**), $[(1,2\text{-}\eta\text{-}^{t}Bu_2P{=}P{-}P^{t}Bu_2)Pd(P^{p}Tol_3)Cl]$ (**2a**), $[(1,2\text{-}\eta\text{-}^{t}Bu_2P{=}P{-}P^{t}Bu_2)Pd(P^{i}Pr_3)Cl]$ (**3b**), $[(1,2\text{-}\eta\text{-}^{t}Bu_2P{=}P{-}P^{t}Bu_2)Ni(PPh_2Et)Cl]$ (**4b**). We have measured the ratios of isomers **a** vs. isomers **b** in reactions solutions and after dissolving the isolated isomer in C_6D_6 (integrations of P3 signals in $^{31}P\{^{1}H\}$ NMR spectra) in room temperature. The ratios are similar (see Table 1). However, after repeated crystallisations we have isolated only one isomer. Thus, an equilibrium according to Scheme 2 is very plausible.

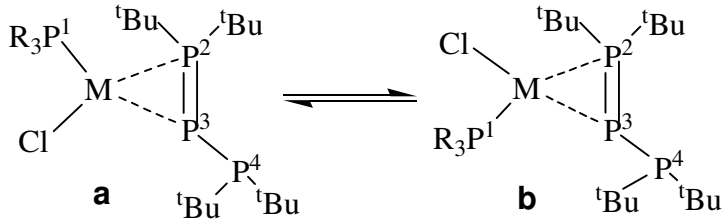

Scheme 2

Table 1. The molar ratio of isomer **a** : isomer **b** of $[(1,2\text{-}\eta\text{-}^{t}Bu_2P{=}P{-}P^{t}Bu_2)M(PR_3)Cl]$ in the reaction solution and in a solution of the isolated complex in C_6D_6.

Isolated isomer	**a** : **b** reaction sol.	**a** : **b** dissolved
$[(1,2\text{-}\eta\text{-}^{t}Bu_2P{=}P{-}P^{t}Bu_2)Pd(PEt_3)Cl]$ (**7a**) [12]	95 : 5	91 : 9
$[(1,2\text{-}\eta\text{-}^{t}Bu_2P{=}P{-}P^{t}Bu_2)Pd(P^{p}Tol_3)Cl]$ (**2a**)	67 : 33	56 : 44
$[(1,2\text{-}\eta\text{-}^{t}Bu_2P{=}P{-}P^{t}Bu_2)Pd(P^{i}Pr_3)Cl]$ (**3b**)	50 : 50	44 : 56
$[(1,2\text{-}\eta\text{-}^{t}Bu_2P{=}P{-}P^{t}Bu_2)Ni(PEt_3)Cl]$ (**8a**) [12]	55 : 45	52 : 48
$[(1,2\text{-}\eta\text{-}^{t}Bu_2P{=}P{-}P^{t}Bu_2)Ni(PPh_2Et)Cl]$ (**4b**)	19 : 81	21 : 79

The reaction according to scheme 1 is accompanied by two main side reactions:

i. Exchange of the R_3P ligand in $[(1,2\text{-}\eta\text{-}^tBu_2P{=}P{-}P^tBu_2)M(PR_3)Cl]$ with $^tBu_2PH$ (Scheme 3). Thus **2a** and **2b** yield **2a*** and **2b*** (equilibrium), **3a** and **3b** yield **2a*** and **2b*** (equilibrium), **4b** yields **4b*.**

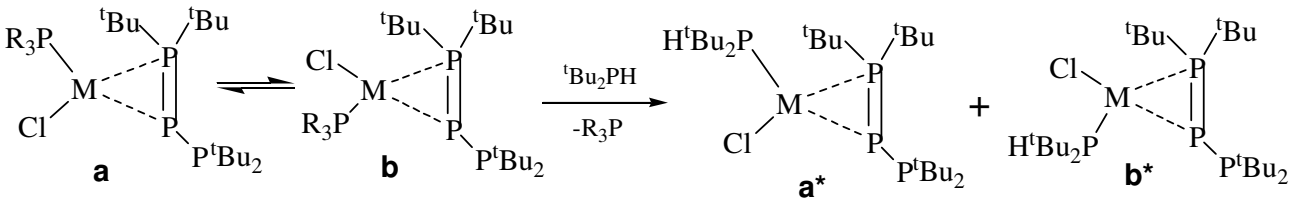

Scheme 3

$^tBu_2PH$ is a product of a splitting of the P–P bond in the triphosphine backbone. Similar splitting was observed and discussed in reactions involving $^tBu_2P{-}P(SiMe_3)Li$ [19].

ii. A reaction leading to formation of a planar isotetraphosphine $(^tBu_2P)_3P$ [23]. A mechanism of its formation is not clear. $(^tBu_2P)_3P$ was found in many runs.

$[(^pTol_3P)_2PtCl_2]$ react with $^tBu_2P{-}PLi{-}P^tBu_2{\cdot}2THF$ forming $[(1,2\text{-}\eta\text{-}^tBu_2P{=}P{-}P^tBu_2)Pt(^pTol_3P)Cl]$ (**1a**) in a poor yield. In the same experiment we have isolated a phosphanylphosphinidene complex $[(\eta^2\text{-}^tBu_2P{=}P)Pt(^pTol_3P)_2]$ [20]. In the reaction solution we have detected a significant amount of $(^tBu_2P)_3P$ and some amount of a Pt complex with four P atoms (**A**). The formation of $(^tBu_2P)_3P$ is not necessary attributed to a formation of $[(\eta^2\text{-}^tBu_2P{=}P)Pt(^pTol_3P)_2]$ since we have not detected this complex in the early stage of run 4.1.

The reaction of $[(Et_3P)_2PtCl_2]$ with $^tBu_2P{-}P(SiMe_3){-}P^tBu_2$ (run 4.2) yields significant amounts of $(^tBu_2P)_3P$. However, we have not detected $[(\eta^2\text{-}^tBu_2P{=}P)Pt(PEt_3)_2]$ which is fairly stable but then $^tBu_2P{-}P{=}PEt_3$ [24]. Moreover, $(^tBu_2P)_3P$ was isolated in a reaction of $[(Et_2PhP)_2PtCl_2]$ with $^tBu_2P{-}PLi{-}P(NEt_2)_2{\cdot}2THF$.

The known complexes $[(1,2\text{-}\eta\text{-}^tBu_2P{=}P{-}P^tBu_2)Pt(PR_3)X]$ (X = Cl, Br) are **a**-type isomers. This fact can be rationalized, taking into account that *trans* influence is most important for heaviest

element in a group [25, 26]. $^{t}Bu_2P2$ (scheme 2) exerts stronger *trans* influence than P3 (see p. 2.2) and it is advantageous to have Cl or Br ligands but not R_3P1 group *trans* to P2 atom

We have studied the reactivity of $^{t}Bu_2P–PLi–P(NEt_2)_2·2THF$ towards a variety of complexes $[(R_3P)_2MCl_2]$ (M = Pt, Pd, Ni). To our surprise these compounds do not react under formation of $[\{1,2\text{-}\eta\text{-}^{t}Bu_2P{=}P–P(NEt_2)_2\}M(PR_3)Cl]$ or $[\{1,2\text{-}\eta\text{-}(Et_2N)_2P{=}P–P^{t}Bu_2)M(PR_3)Cl]$. We have isolated and identified only two known compounds and a new adduct of $^{t}Bu_2P–PLi–P(NEt_2)_2$.

1. $(^{t}Bu_2P)_3P$ in a reaction of $^{t}Bu_2P–PLi–P(NEt_2)_2·2THF$ with $[(Et_2PPh)_2NiCl_2]$.

2. $[\mu\text{-}(1,3{:}2,3\text{-}\eta\text{-}^{t}Bu_2P_4{}^{t}Bu_2)\{Ni(PEt_3)Cl\}_2]$ (**5**) [27] together with two other compounds **B** [27] and **C** in a reaction of $^{t}Bu_2P–PLi–P(NEt_2)_2·2THF$ with $[(Et_3P)_2NiCl_2]$.

3. $^{t}Bu_2P–PLi–P(NEt_2)_2·2THF$ react with $[(Et_2PhP)_2PtCl_2]$ yielded oily product and $(^{t}Bu_2P)_3P$ (not detected in the early stage of this reaction). $^{t}Bu_2P–PLi–P(NEt_2)_2·2THF$ was converted to relatively inert $LiCl·2\{^{t}Bu_2P–PLi–P(NEt_2)_2\}·2THF$ [28]. This compound does not dissociate into $^{t}Bu_2P–PLi–P(NEt_2)_2$ in THF solution.

The formation of **5** and of $(^{t}Bu_2P)_3P$ indicates a splitting of the $P–P(NEt_2)_2$ bond in the parent triphosphine backbone.

2.2. ^{31}P-NMR Studies, X-Ray Crystallographic Studies and Discussion

In Table 2 are collected $^{31}P\{^{1}H\}$ MNR data for complexes with side-on bonded $^{t}Bu_2P{=}P–P^{t}Bu_2$ ligand. These data indicate that the structures in solution are the same as in solid state. The equilibrium according to Scheme 2 is slow in the NMR time scale and we observed separated resonances for all isomers. The large absolute values of the couplings constants $^{1}J_{P2\text{-}P3}$ of 560/518 Hz (M = Pd, Ni) and 482/447 (M = Pt) show that this bond has a multiple bond character. Noteworthy is a substantial high field shift of P3 (–66 / –130 ppm) indicating a single-bond character of a Pt-P3 bond. Similar features displays side-on bonded $^{t}Bu(Cl)P{=}P–^{t}Bu$ connected to $CpW(CO)_2$ centre [29]. The values of *trans* ^{2}JP1-P2 in "**b**" complexes are in the range 249.9/270 Hz (M = Pd) and 178.3/194.3 Hz (M = Ni). In "**a**" complexes **t**he values of *trans* ^{2}JP1-P3 are in the

range 102.9/108.5 Hz (M = Pt, Pd) and 75.6/75.8 (M = Ni). Thus the *trans* influence of P2 is stronger than that of P3. This assumption is additionally supported by the values of ^{1}JPt-P in **1a**. The ^{1}JPt-P1 *trans* to P3 is 3437.3 Hz and is similar to the ^{1}JPt-P coupling in [*cis*-(^{p}Tol3P)2PtCl2] of 3627 Hz. Thus according to the criterion of Benett [30] P3 atom exerts very low *trans* influence, similar to that of a Cl atom.

Table 2. ^{31}P{^{1}H) NM(R data for [(1,2-η-^{t}Bu$_2$P=P–P^{t}Bu$_2$)M(PR$_3$)Cl] (M = Ni , Pd)

	M	R_3P1	δ P1 ppm	δ P2 ppm	δ P3 ppm	δ P4 ppm	J_{P1-P2} Hz	J_{P1-P3} Hz	J_{P1-P4} Hz	J_{P2-P3} Hz	J_{P2-P4} Hz	J_{P3-P4} Hz
1a	Pt	^{p}Tol$_3$P	26.2	62.4	-130.4	27.8	20.7	107.8		447.3	32.6	254.7
6a[a]	Pt	Ph$_3$P	28.0	61.0	-125.9	32.0	22.0	107.0		482.0	34.0	251.0
2a	Pd	^{p}Tol$_3$P	20.1	105.5	-87.7	28.7	25.2	103.3		549.7	33.2	246.7
2b	Pd	^{p}Tol$_3$P	15.9	97.2	-65.7	33.3	265.1	13.8		539.2	36.7	247.8
2a*	Pd	^{t}Bu$_2$H	30.7	104.2	-89.7	26.8	25.5	104.1		557.6	32.1	248.9
2b*	Pd	^{t}Bu$_2$H	41.8[b]	75.6	-66.2	26.9	251.2	16.1	2.2	547.3	32.1	242.1
3a	Pd	^{i}Pr$_3$P	47.7	100.8	-88.4	31.0	23.0	102.9		551.7	30.3	255.2
3b	Pd	^{i}Pr$_3$P	35.5	77.2	-74.8	32.5	249.9	16.2		535.8	30.3	255.1
7a[c]	Pd	Et$_3$P	22.6	110.3	-103.4	26.2	21.7	108.5		550.8	33.5	248.0
7b[c]	Pd	Et$_3$P	10.7	79.2	-74.5	28.8	270.0	15.3		534.0	34.9	241.0
4a	Ni	Ph$_2$Et	21.4	69.9	-119.2	32.7	30.2	75.8		531.6	25.5	257.0
4b	Ni	Ph$_2$Et	13.6	39.5	-97.5	36.4	191.0	≈ 0		523.5	29.4	253.6
4b*	Ni	^{t}Bu$_2$H	40.4	22.9	-90.6	32.0	178.3	≈ 0	2.2	538.5	22.3	255.1
8a[c]	Ni	Et$_3$P	19.9	72.8	-127.8	31.8	33.4	75.6		531.6	26.4	256.3
8b[d,c]	Ni	Et$_3$P	7.1	31.3	-101.8	34.1	194.3	2.4		518.0	27.8	252.8

[a] – see [13] , Br in place of Cl, [b] – $^{1}J_{P1-H}$ = 286 Hz, [c] – see [12], [d] – higher order spectrum

The structures of **1a·pentane** (Fig. 1), **2a** (Fig. 2), **3b** (Fig. 3) and **4b** (Fig. 4) were determined by X-ray diffraction methods [31, 32]. The crystal data, details of the data collection and refinement are given in Table 3.

The Pt atom in **1a** (RMS deviations of fitted atoms = 1.69 pm) and the Pd atom in **2a** (RMS deviations = 1.10 pm) are in an almost planar environment defined by R_3P1, Cl and the P2–P3 bond. In **3b** (RMS deviations = 5.46 pm) the environment around Pd atom displays small deviations from planarity and in **4b** (RMS deviations = 23.7 pm) the environment around Ni atom displays substantial deviations from planarity. The P2-P3 distances are short: 214.50(2) pm in **1a**,

213.03(13) pm in **2a**, 213.32(7) pm in **3b** and 212.54 (12) pm in **4b**. These data and literature data for **6a** – 214.9(2) pm [22], for **7a** – 213.68(5) pm [21] and for **8a** – 212.81(10) pm [21] indicate general trend that the distances P2-P3 diminish in the order Pt > Pd > Ni. These short distances are typical for the double P=P bond of diphosphenes upon η^2-coordination [33]. All P3-P4 distances are in the range of single P–P bonds [34].

Table 3. Summary of crystallographic data and structure refinement details for **1a-4b.**

	1a	2a	3b	4b
Empirical formula	$C_{42}H_{69}ClP_4Pt$	$C_{37}H_{57}ClP_4Pd$	$C_{25}H_{57}ClP_4Pd$	$C_{30}H_{51}ClP_4Ni$
M_r /g mol^{-1}	928.39	767.56	623.44	629.75
Temperature /K	120(2)	120(2)	120(2)	120(2)
Wavelength /Å	0.71073 (Mo K_α)	0.71073 (Mo K_α)	0.71073 (Mo K_α)	0.71073 (Mo K_α)
Crystal system	monoclinic	triclinic	triclinic	monoclinic
Space group	$P2_1/c$	P -1	P -1	$P2_1/c$
a /Å	14.7717(4)	11.9728(5)	8.4306(4)	8.2709(4)
b /Å	24.5098(6)	12.7680(5)	11.8235(4)	19.6137(12)
c /Å	13.2810(3)	14.2078(9)	16.9039(6)	20.2758(12)
α/°	90	93.391(4)	89.747(3)	90
β /°	110.902(2)	114.571(4)	91.967(3)	93.444(4)
γ/°	90	98.813(3)	108.684(4)	90
V /Å^3	4491.97(19)	1933.61(17)	1595.19(10)	3283.3(3)
Z	4	2	2	4
Calc. density /Mg m^{-3}	1.373	1.318	1.298	1.274
Crystal size / mm	0.26 × 0.24 × 0.15	0.08 × 0.06 × 0.02	0.16 × 0.09 × 0.02	0.10 × 0.05 × 0.02
θ range /°	1.96 to 25.5	1.91 to 25.5	2.17 to 25.5	2.26 to 25.5
Limiting indices	–17<=h<=17	–13<=h<=14	–10<=h<=10	–10<=h<=10
	–27<=k<=29	–15<=k<=15	–14<=k<=13	–23<=k<=21
	–16<=l<=16	–16<=l<=17	–20<=l<=20	–24<=l<=24
Reflections collected /	31323 / 8354	14073 / 7206	11626 / 5947	23453 / 6098
unique	[R(int) = 0.0565]	[R(int) = 0.0394]	[R(int) = 0.0226]	[R(int) = 0.0706]
Completeness to	100	99.8	99.8	100
θ_{max} /%				
Linear absorption coeff.	3.352	0.738	0.878	0.885
/mm^{-1}				
Data / restraints /	8354 / 0 /450	7206 / 0 / 403	5947 / 0 / 298	6098 / 0 / 338
parameters				
Goodness–of–fit on F^2	1.16	1.041	1.151	0.932
Final R indices [I>2σ(I)]	$R1$ = 0.0501	$R1$ = 0.0379	$R1$ = 0.0253	$R1$ = 0.0412
	$wR2$ = 0.1228	$wR2$ = 0.0949	$wR2$ = 0.0645	$wR2$ = 0.0917
R indices (all data)	$R1$ = 0.0712	$R1$ = 0.0543	$R1$ = 0.0308	$R1$ = 0.0737
	$wR2$ = 0.1393	$wR2$ = 0.1077	$wR2$ = 0.067	$wR2$ = 0.0978
Largest diff. peak and	1.576 and	0.703 and	0.588 and	0.559 and
hole /eÅ^{-3}	–1.146	–0.67	–0.627	–0.607

The M–P distances display distinct differences depending on the isomer type. In **3b** the Pd–P1 distance 234.32 (9) pm, *trans* to P2 is longer than 236.03 pm reported for Pd–P bond in [*trans*-($^{i}Pr_3P)_2PdCl_2$] [35]. Thus $^{t}Bu_2P2$ exerts strong *trans* influence. Pd–P2 bond is very short - 225.39(15) pm, similarly to 225.8 (3) reported for Pd–P bond in [*cis*-$(Me_3P)_2PdCl_2$] [36], however, it has $^{i}Pr_3P1$ in *trans* position. The Pd–P3 bond of 238.59(5) pm *trans* to Cl atom is a long one. In **2a** Pd–P1 (234.32 (9) pm) is shorter than in **3b** (238.77(5) pm)- but Pd–P3 bond of 241.79 (9) pm, *trans* to $^{p}Tol_3P$ is a very long one. Thus, P3 exerts small *trans* influence but the Pd–P3 bond lengthens very significantly if a tertiary phosphine is in *trans* position to it. The same was observed in Ni complexes **4b** and **8a**.

FIGURE 1. An ORTEP view of the molecular structure of **1a** in the crystal; hydrogen atoms not shown, ellipsoids are drawn at 30% probability level. Selected bond lengths [pm] and angles [°]: Pt1-Cl1 236.37(15); Pt1-P1 228.53(17); Pt1-P2 221.24(16); Pt1-P3 240.77(18); P2-P3 214.50(2); P3-P4 221.80(3); P2-Pt1-P3 55.14(6); P2-P3-P4 106.92(10).

FIGURE 2. An ORTEP view of the molecular structure of **2a** in the crystal; hydrogen atoms not shown, ellipsoids are drawn at 30% probability level. Selected bond lengths [pm] and angles [°]: Pd1-Cl1 238.62(9); Pd1-P1 234.32(9); Pd1-P2 223.15(9); Pd1-P3 241.79(9); P2-P3 213.03(13); P3-P4 222.40(13); P2-Pd1-P3 67.28(4); P2-P3-P4 106.78(5).

FIGURE 3. An ORTEP view of the molecular structure of **3b** in the crystal; hydrogen atoms not shown, ellipsoids are drawn at 30% probability level. Selected bond lengths [pm] and angles [°]: Pd1-Cl1 237.63(5); Pd1-P1 238.77(5); Pd1-P2 225.39(5); Pd1-P3 238.59(5); P2-P3 213.32(7); P3-P4 224.05(7); P2-Pd1-P3 54.654(17); P2-P3-P4 102.96(3).

FIGURE 4. An ORTEP view of the molecular structure of **4b** in the crystal; hydrogen atoms not shown, ellipsoids are drawn at 30% probability level. Selected bond lengths [pm] and angles [°]: Ni1-Cl1 220.46(9); Ni1-P1 223.68(10); Ni1-P2 214.83(10); Ni1-P3 226.05(10); P2-P3 212.54(12); P3-P4 224.80(12); P2-Ni1-P3 57.58(3); P2-P3-P4 105.58(5).

In **1a** the Pt-P2, Pt-P3 and Pt-Cl distances are very similar to those reported in **2a** (M =Pd), however the Pt–P1 distance of 228.53 (7) pm is shorter than Pd–P1 distance in **2a**. We have suggested [21] two Lewis structures which partially explain properties of this class of complexes. The features of X-ray structures are well explained by the Lewis structure 1 (Scheme 4) .

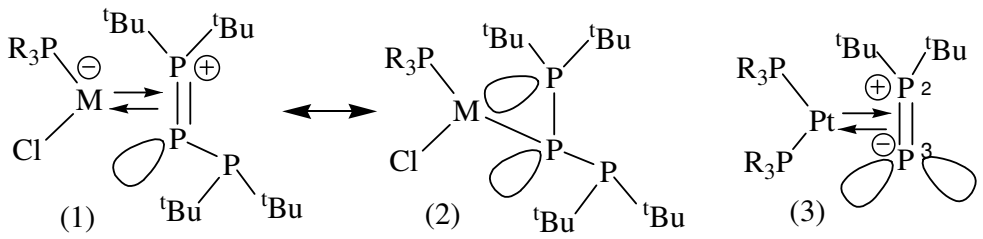

Scheme 4

The planar alignments around the metal centres in all this compounds are in accord with assumption that $(R_3P)ClM^-$ groups exhibit properties of a d^{10} ML_2 metal centre [37] and so this ligand can be seen as an η^2 bonded 1,1-di-*tert*-butyl-2-(di-*tert*-butylphosphanylo)diphosphenium cation. Related phosphanylophosphenium cation has a planar geometry [38]. The short distances M–P^tBu_2 (Scheme 4, structure 1) are due to additional electrostatic interactions. Such interactions are not possible in side-on bonded phosphanylphosphinidene platinum complexes (Scheme 4, structure 3). Thus the Pt–P^tBu_2 distance in $[(^pTol_3P)_2Pt(\eta^2\text{-}^tBu_2P{=}P)]$ is 230.59(17) pm [20] compared to Pt-P2 in **1a** - 221.24 (16) pm. This distance is shorter than Pt–P^tBu_2H distance in $[cis\text{-}(Ph_3P)(^tBu_2PH)PtCl_2]$ (225.3 pm) [39]. These additional electrostatic interactions may be partially responsible for a greater value of $^1J_{Pt\text{-}P2}$ in **1a** compared to $[(^pTol_3P)_2Pt(\eta^2\text{-}^tBu_2P{=}P)]$ [20]. The geometry around P3 atom differs to some extent from the geometry of side-on bonded diphosphenes. The P4-P3-P2 angle in **1a** of 106.71 deg differs slightly from the related angle in $[(\eta^2\text{-}^tBu_2P\text{-}P{=}P\text{-}P^tBu_2)Pt(PPh_3)_2]$ – 111.12 deg. The torsion angle Pt-P2-P3-P4 of 107.12 deg differs from the related value in $[(\eta^2\text{-}^tBu_2P\text{-}P{=}P\text{-}P^tBu_2)Pt(PPh_3)_2]$ – 103.82 deg [33]. The sum of angles around $^pTol_3$**P1** in **1a** is 312.67 deg. The sum of angles around $^tBu_2$**P2**–P is 344.62 deg. Thus the geometry around P2 atom is more planar than around P1 atom. The Lewis structure 2 (Scheme 4) explains the relatively large $^1J_{Pt\text{-}P2}$

(2776.8 Hz for **1a** and 2740 Hz for **6a**). These values of $^{1}J_{Pt\text{-}P3}$ of 187.0 Hz[1] (**6a**) and 188.1 Hz (**1a**) are however smaller than reported for $^{t}Bu_2P–P=P–P^{t}Bu_2$ bonded side-on to d^{10} PtL_2 centre (332 / 404 Hz) [33] and significantly smaller than in terminal phosphido complexes with tertiary phosphine in trans position (573Hz / 675 [15], 806 / 1239 Hz [17]) but greater than in complexes with $^{t}Bu_2P=P$ bonded side-on to d^{10} PtL_2 centre (32 / 104 Hz) [40]. The planar geometry of P1-Cl-P2-P3-M in Lewis structure 2 (Scheme 4) is obvious in terms of the planarity of low spin d^8 ML_2 complexes.

The crystallographic data have been deposited in the Cambridge Crystallographic Data Centre as supplementary publications CCDC 746220 (**1a·pentane**), CCDC 746221 (**2a**), CCDC 746222 (**3b**) and CCDC 746223 (**4b**). Copies of the data can be obtained free of charge on application to the Director CCDC, 12 Union Road, Cambridge CB21EZ, UK (fax: +(44) 1223-336-033; e-mail for inquiring: fileserv@ccdc.cam.ac.uk , e-mail for deposition: deposit@ccdc.cam.ac.uk

3. Conclusion

We have isolated several new complexes $[(1,2\text{-}\eta\text{-}^{t}Bu_2P=P–P^{t}Bu_2)M(PR_3)Cl]$ which are products of reactions of $[(R_3P)_2MCl_2]$ with $^{t}Bu_2P–PLi–P^{t}Bu_2$. In solution we observed a mixture of isomers in an equilibrium. For $[(^{p}Tol_3P)_2PtCl_2]$ only one isomer of $[(1,2\text{-}\eta\text{-}^{t}Bu_2P=P–P^{t}Bu_2)Pt(PR_3)Cl]$ was formed together with a phosphanylophosphinidene complex $[(\eta^2\text{-}^{t}Bu_2P=P)Pt(P^{p}Tol_{32})_2]$. The studied reactions are not general for lithiated triphosphines and were successful only for a compound with voluminous ^{t}Bu groups. Surprisingly $^{t}Bu_2P–PLi–P(N^{i}Pr_2)_2$ does not form related complexes with $1,2\text{-}\eta\text{-}^{t}Bu_2P=P–P(N^{i}Pr_2)_2$ or $2,3\text{-}\eta\text{-}^{t}Bu_2P–P=P(N^{i}Pr_2)_2$ ligands but a splitting of a $P–P(N^{i}Pr_2)_2$ was observed. It seems reasonable to study related reactions involving lithiated triphospines with smaller groups e. i. $^{i}Pr_2P–PLi–P^{i}Pr_2$.

[1] The value 95 Hz previously reported [21, 22] was a mistake.

4. Experimental

All manipulations were performed in flame-dried Schlenk type glassware on a vacuum line. THF and toluene were dried over Na/benzophenone and distilled under nitrogen. Pentane was dried over Na/benzophenone/diglyme and distilled under nitrogen. ^{31}P NMR spectra were recorded on Bruker Av400 and on Bruker AMX300 spectrometers (external standard 85% H_3PO_4) at ambient temperature. The ^{1}H NMR signals for **2a**, **2b** and **3b** were established from ^{31}P-^{1}H-COSY spectra. $^{t}Bu_2P–P(SiMe_3)–P^{t}Bu_2$ was prepared in a one-pot reaction [41] and lithiated according to literature procedures [42], $^{t}Bu_2P–PLi–P(NEt_2)_2$ was prepared according to literature procedures [43]

*4.1. Reaction of $^{t}Bu_2P–PLi–P^{t}Bu_2·2THF$ with $[^{p}Tol_3P)_2PtCl_2]$. Synthesis of $[(1,2-\eta-^{t}Bu_2P=P–P^{t}Bu_2)Pt(p-Tol_3P)Cl]$ (**1a**).*

A solution of $^{t}Bu_2P–PLi–P^{t}Bu_2·2THF$ (0.187 g, 0.396 mmol) in THF (2 mL) was added at room temperature to a suspension of [*cis/trans*-$(^{p}Tol_3P)_2PtCl_2$] (0.346 g, 0.396 mmol) in THF (2 mL). The mixture was stirred for 1 d, the suspension dissolved (the solution turned orange) and was investigated with ^{31}P{^{1}H} NMR, then evacuated at $2·10^{-3}$ Torr for 2 h. The residue was dissolved in toluene (4 mL) and filtered. The volume was reduced to ≈ 1 mL and pentane (4 mL) was carefully layered over the toluene solution. After 7 days at + 4 ^{o}C orange crystals of **1a·pentane** deposited (0.079 g, 21 % yield). Then the mother liquor was separated from crystals and after 7 days at + 4 ^{o}C yielded small amount of red crystals of $[(\eta^2-^{t}Bu_2P=P)Pt(p-Tol_3P)_2]$ [20]

^{31}P-NMR examination of reaction solution: **1a**, $(^{t}Bu_2P)_3P$ [23], [*cis*-(*p*-Tol_3P)($^{t}Bu_2PH$)$PtCl_2$], $^{t}Bu_2P–PH–P^{t}Bu_2$ [41], *p*-Tol_3P, **A**.

1a : ^{31}P{^{1}H} NMR (161.94 MHz, MHz, C_6D_6, THF, 25 ^{o}C,) δ = 26.2 (dd, P1); 62.4 (ddd, P2); –130.4 (ddd, P3); 27.8 (dd, P4); $^{1}J_{Pt-P1}$ = 3437.3 Hz, $^{1}J_{Pt-P2}$ = 2776.8 Hz, $^{1}J_{Pt-P3}$ = 188.1Hz, $^{1}J_{Pt-P4}$ = 45.9 Hz, $^{2}J_{P1-P2}$ = 20.7 Hz, $^{2}J_{P1-P3}$ = 107.8 Hz, $^{3}J_{P1-P4}$ ≈ 0 Hz, $^{1}J_{P2-P3}$ = –447.3 Hz, $^{2}J_{P2-P4}$ = 32.6 Hz, $^{1}J_{P3-P4}$ = –254.7 Hz.

A : $^{31}P\{^1H\}$ NMR (161.94 MHz, MHz, C_6D_6, THF, 25 ^oC,) δ = 22.0 (ddd, P1); –14.1 (dd, P2); –32.0 (ddd, P3); –45.4 (ddd, P4); $^1J_{Pt-P1}$ = 2547.0 Hz, $^1J_{Pt-P2}$ = 2161.5 Hz, $^1J_{Pt-P3}$ = 1454.6Hz, $^1J_{Pt-P4}$ ≈ 20 Hz, J_{P1-P2} = 315.6 Hz, J_{P1-P3} = 12.7 Hz, J_{P1-P4} = 6.7 Hz, J_{P2-P4} = 323.5 Hz, J_{P2-P3} = 9.2 Hz, J_{P3-P4} = 275.3 Hz, $^1J_{P3-H}$ = 165.0 Hz..

[*cis*-(^{p}Tol$_3$P2)(^{t}Bu$_2$P1H)PtCl$_2$] $^{31}P\{^1H\}$ NMR (161.94 MHz, C_6D_6, THF, 25 ^oC,) δ = 50.4 (d, P1); 13.3 (d, P2); $^1J_{Pt-P1}$ = 3502 Hz, $^1J_{Pt-P2}$ = 3668 Hz, $^2J_{P1-P2}$ = 10.6 Hz,

4.2. Reaction of ^{t}Bu$_2$P–P(SiMe$_3$)–P^{t}Bu$_2$ with [(Et$_3$P)$_2$PtCl$_2$].

A solution of ^{t}Bu$_2$P–P(SiMe$_3$)–P^{t}Bu$_2$ (0.11 g, 0.28 mmol) in THF (2 mL) was added at room temperature to a solution of [*cis/trans*-(Et$_3$P)$_2$PtCl$_2$] (0.14 g, 0.28 mmol) in THF (7 mL). The mixture turned slowly yellow. After 1 d the solution was concentrated to 2 mL and colourless crystals of (^{t}Bu$_2$P)$_3$P deposited.

^{31}P-NMR examination of reaction solution (101.26 MHz, C_6D_6, THF, 25 ^oC): (^{t}Bu$_2$P)$_3$P [23], [*cis*-(Et$_3$P)(^{t}Bu$_2$PH)PtCl$_2$], ^{t}Bu$_2$PH, *p*-Tol$_3$P, [*cis*-(Et$_3$P)$_2$PtCl$_2$], [*trans*-(Et$_3$P)$_2$PtCl$_2$], ^{t}Bu$_2$P–P=PEt$_3$ [24] [*cis*-(Et$_3$P2)(^{t}Bu$_2$P1H)PtCl$_2$] $^{31}P\{^1H\}$ NMR (101.26 MHz, C_6D_6, THF, 25 ^oC,) δ = 34.4 (d, P1) ; 4.7 ppm (d, P2) ; $^1J_{Pt-P1}$ = 3531.0 Hz, $^1J_{Pt-P2}$ = 3365.8 Hz, $^2J_{P1-P2}$ = 15.4 Hz,

*4.3. Reaction of ^{t}Bu$_2$P–PLi–P^{t}Bu$_2$·2THF with [(^{p}Tol$_3$P)$_2$PdCl$_2$]. Synthesis of [(1,2-η-^{t}Bu$_2$P=P–P^{t}Bu$_2$)Pd(P^{p}Tol$_3$)Cl] (**2a**).*

A solution of ^{t}Bu$_2$P–PLi–P^{t}Bu$_2$·2THF (0.210 g, 0.444 mmol) in THF (2 mL) was added at room temperature to a suspension of [(^{p}Tol$_3$P)$_2$PdCl$_2$] (0.349 g, 0.444 mmol) in THF (2 mL). The yellow suspension turned immediately dark red. After stirring for 2 h the suspension dissolved and volume was reduced to 2 mL. The reaction mixture was investigated by $^{31}P\{^1H\}$ NMR. Then the solution was evaporated to dryness under *vacuum*, dissolved in toluene (4 mL) filtrated, concentrated to 1 mL and stored for 5 d at 4 ^oC. Crystals of ^{p}Tol$_3$P were deposited. Then the solution was stored for

14 d at –35 ºC. The pale yellow crystals of $(^tBu_2P)_3P$ were deposited. The resulting mother liquor was layered with pentane. After 14 d at 4 ^oC orange needles of **2a** deposited (0.106g, 31% yield).

^{31}P-MNR examination of reaction solution. **2a**, **2b**, **2a*** (small signals), **2b*** (small signals), $^tBu_2P$–PH–P^tBu_2 (small signals) and $(^tBu_2P)_3P$ (small signals).

2a : ^{1}H NMR (400.13 MHz, C_6D_6, 25 ^oC): δ = 7.91 (m, *o*-H of C_7H_7P1 of **2a** or **2b;** 6.94 (m, probably *m*-H of C_7H_7P1 of **2a** or **2b**, overlap with *p*-Tol_3P) ; 2.003 (s, CH_3 of *p*-Tol_3P1 of **2a** or **2b**); 1.991 (s, CH_3 of *p*-Tol_3P1 of **2a** or **2b**); 1.902 (d, 11.9 Hz, $\mathbf{H_3}$CCP4); 1.386 (d, 10.7 Hz, $\mathbf{H_3}$CCP4); 1.282 (d, 16.6 Hz, $\mathbf{H_3}$CCP2); 1.148 (d, 15.2 Hz, $\mathbf{H_3}$CCP2);

2b : ^{1}H NMR (400.13 MHz, C_6D_6, 25 ^oC):): δ = 7.91 (m, *o*-H of C_7H_7P1 of **2a** or **2b;** 6.94 (m, probably *m*-H of C_7H_7P1 of **2a** or **2b**, overlap with *p*-Tol_3P) ; 2.003 (s, CH_3 of *p*-Tol_3P1 of **2a** or **2b**); 1.991 (s, CH_3 of *p*-Tol_3P1 of **2a** or **2b**); 1.829 (d, 17.1 Hz, $\mathbf{H_3}$CCP2); 1.508 (d, 13.8 Hz, $\mathbf{H_3}$CCP2); 1.464 (d, 10.7 Hz, $\mathbf{H_3}$CCP4); 1.082(d, 11.5 Hz, $\mathbf{H_3}$CCP4);

*4.4. Reaction of $^tBu_2P$–PLi–P^tBu_2·2THF with $[(^iPr_3P)_2PdCl_2]$. Synthesis of $[(1,2\text{-}\eta\text{-}^tBu_2P{=}P\text{–}P^tBu_2)Pd(P^iPr_3)Cl]$ (**3b**).*

A solution of $^tBu_2P$–PLi–P^tBu_2·2THF (0.208 g, 0.440 mmol) in THF (3 mL) was added at room temperature to a suspension of $[(^iPr_3P)_2PdCl_2]$ (0.219 g, 0.440 mmol) in THF (2 mL). The yellow solution turned orange-brown. After stirring for 1 h the suspension dissolved volume was reduced to 2 mL and investigated by $^{31}P\{^1H\}$ NMR. Then the solution was evaporated to dryness under *vacuum*, dissolved in toluene (4 mL) filtrated and concentrated to 1 ml. The solution was layered with pentane (4mL) and stored for 7 d at 4 ^oC. Orange crystals deposited: **3b** (0.160g, 58% yield).

^{31}P-MNR examination of reaction solution: **3a**, **3b**, **2a***, **2b***, $^tBu_2P$–PH–P^tBu_2, $^tBu_2PH$ and $[(^iPr_3P)_2PdCl_2]$ were found.

3a: ^{1}H NMR (400.13 MHz, C_6D_6, 25 ^oC): 1.773 (d, 12.0 Hz, $\mathbf{H_3}$CCP4); 1.576 (dd, 1.1 Hz + 16.0 Hz, $\mathbf{H_3}$CCP2); 1.453 (d, 10.5 Hz, $\mathbf{H_3}$CCP4); Others signals we were not able to assign unequivocally to H atoms of **3a**.

3b: ^{1}H NMR (400.13 MHz, C_6D_6, 25 ^{o}C): 1.389 (d, 11.0 Hz, **H$_3$**CCP4); Others signals we were not able to assign unequivocally to H atoms of **3b**.

*4.5. Reaction of $^{t}Bu_2P–PLi–P^{t}Bu_2·2THF$ with $[(Ph_2EtP)_2NiCl_2]$. Synthesis of $[(1,2-\eta-^{t}Bu_2P=P–P^{t}Bu_2)Ni(PPh_2Et)Cl]$ (**4b**).*

A solution of $^{t}Bu_2P–PLi–P^{t}Bu_2·2THF$ (0.210 g, 0.444 mmol) in THF (2 mL) was added at room temperature to a suspension of $[(Ph_2EtP)_2NiCl_2]$ (0.248 g, 0.444 mmol) in THF (2 mL). The cherry-red solution turned red-brown and the suspension dissolved. Then the solution was evaporated to dryness under *vacuum*, dissolved in toluene (4 mL) filtrated and concentrated to 1 ml. Pentane (4mL) was put over the toluene solution and the bulb was stored for 5 d at 4 ^{o}C. Cherry-red crystals deposited: **4b,** (0.212 g, 76% yield)

^{31}P-MNR examination of reaction solution: **4a**, **4b**, $[(1,2-\eta-^{t}Bu_2P=P–P^{t}Bu_2)Ni(P^{t}Bu_2H)Cl]$ (**4b*),** $^{t}Bu_2P–PH–P^{t}Bu_2$, $^{t}Bu_2PH$, $^{t}Bu_2PCl$ and Ph_2EtP were found.

*4.6. Reaction of $^{t}Bu_2P–PLi–P(NEt_2)_2·2THF$ with $[(Et_3P)_2NiCl_2]$. Synthesis of $[\mu-(1,3:2,3-\eta-^{t}Bu_2P_4{}^{t}Bu_2)\{Ni(PEt_3)Cl\}_2]$(**5**)*

A solution of $^{t}Bu_2P–PLi–P(NEt_2)_2·2THF$ (0.271 g, 0.539 mmol) in THF (2 mL) was added at room temperature to a suspension of $[(Et_3P)_2NiCl_2]$ (0.193 g, 0.527 mmol) in THF (2 mL). The cherry-red solution turned red-brown and the suspension dissolved. Then the solution was evaporated to dryness under *vacuum*, dissolved in toluene (4 mL) filtrated and concentrated to 1 ml. Pentane (5mL) was put over the toluene solution and the bulb was stored for one week at –35 ^{o}C. Small amount of cherry-red crystals of **5** was deposited (0.049g).

^{31}P-MNR examination of reaction solution: **5** [18], **B** [18], **C**, $(Et_2N)_3P$, $^{t}Bu_2PH$, $^{t}Bu_2P–P=PEt_3$ and Et_3P were found.

5 : $^{31}P\{^{1}H\}$ NMR (101.26 MHz, Tol, C_6D_6, 25 ^{o}C,) δ = –28.5 (dddd, P1); –1.0 (dddd, P2), –94.6 (ddddd, P3), 70.6 (m, P4), 5.0 (ddd, P5), 8.6 (m, P6), J_{P1-P2} = 197.8, J_{P1-P3} = 89.2, J_{P1-P4} =

10.5, J_{P1-P5} = 292.2, J_{P1-P6} = 2.2, J_{P2-P3} = 298.5, J_{P2-P4} = 11.8, J_{P2-P5} = 1.9, J_{P3-P4} = 511.3, J_{P3-P5} = 64.8, J_{P3-P6} = 187.5, J_{P4-P5} = 2.5, J_{P4-P6} = 8.0, J_{P5-P6} = 10.5.

B : $^{31}P\{^{1}H\}$ NMR (101.26 MHz, Tol, C_6D_6, 25 ^{o}C,) δ = 64.0 (dddd, P1); 12.1 (dd P2), –8.7 (ddddd, P3), –126.2 (ddddd, P4), –157.7 (dddd, P5), –182.1 (dddd, P6), J_{P1-P2} = 3.9, J_{P1-P3} = 28.4, J_{P1-P4} = 85.0, J_{P1-P5} = 162.3, J_{P1-P6} = 196.9, J_{P2-P3} = 283.3, J_{P2-P4} = 32.8, J_{P2-P5} = 2.2, J_{P2-P6} = 2.8, J_{P3-P4} = 19.5, J_{P3-P5} = 180.5, J_{P3-P6} = 60.1, J_{P4-P5} = 119.9, J_{P4-P6} = 210.8, J_{P5-P6} = 172.2 [18].

C : $^{31}P\{^{1}H\}$ NMR (161.94 MHz, THF, C_6D_6, 25 ^{o}C,) δ = 49.6 (dddd, P1); 13.2 (dd dP2), 8.3 (ddd, P3), –6.2 (ddd, P4), –38.9 (ddd, P5), J_{P1-P2} = 84.9, J_{P1-P3} = 227.6, J_{P1-P4} = 134.2, J_{P1-P5} = 289.1, J_{P2-P3} = 16.0, J_{P2-P4} = 256.8, J_{P3-P5} = 13.8, J_{P4-P5} = 193.8,

Crystallographic refinement details. Diffraction data were recorded on a KUMA KM4 diffractometer with graphite-monochromated Mo K_α radiation using Sapphire-2 CCD detector (Oxford Diffraction Ltd). The apparatus was equipped with an open flow thermostat (Oxford Cryosystems) which enabled experiments at 120K. The structures were solved with direct methods and refined with the SHELX97 program package[30] with the full-matrix least-squares refinement based on F^2. The data were corrected for absorption with the CrysAlis RED program. All non-hydrogen atoms were refined anisotropically. All H atoms were positioned geometrically and refined using a riding model C—H = 0.95 – 0.99 Å and U_{iso}(H) =1.2U_{eq}(C) or 1.5 U_{eq} (C) for CH_3 groups.

Acknowledgements

J.P. and R.G thank the Polish Ministry of Science and Higher Education (Grant Nr N N204 271535) for financial support.

References

[1] R. Waterman, Dalton Trans. **2009,** 18

[2] H. Schäfer, Z. Anorg. Allg. Chem. **1979**, 459, 129.

[3] H. Schäfer, Z. Naturforsch. **1979**, 34B, 1358.

[4] B. Deppisch, H. Schäfer, Z. Anorg. Allg. Chem. **1982**, 490, 129.

[5] H. Schäfer, Acta Cryst. **1982**, 38B, 748.

[6] H. Schäfer, D. Binder, Z. Anorg. Allg. Chem. **1987**, 546, 55.

[7] H. Schäfer, D. Binder, D. Fenske, Angew. Chem. **1985**, 97, 523; b) Angew. Chem. Int. Ed. **1985**, 24, 522.

[8] H. Schäfer, D. Binder, B. Deppisch, G. Mattern, Z. Anorg. Allg. Chem. **1987**, 546, 79.

[9] R. A. Jones, A. L. Stuart, J. L. Atwood, W. E. Hunter, Organometallics **1983**, 2, 874.

[10] M. Driess, H. Pritzkow, U. Winkler, J. Organomet. Chem., **1997**, 529, 313

[11] R. Melenkivitz, D. J. Mindiola, G. L. Hillhouse, J. Am. Chem. Soc., **2002**, 124, 3846

[12] R. Giannandrea, P. Mastrorilli, C.F. Nobile, U. Englert, J. Chem. Soc. Dalton, **1997**, 1355

[13] U. Englert, E. Matern, J. Olkowska-Oetzel, J. Pikies. Acta Cryst. **2003**, E59, m376

[14] M. A. Zhuravel, D. S. Glueck, L. N. Zakharov, A. L. Rheingold. Organometallics, **2002**, 21, 3208

[15] H. Schäfer, D. Binder, Z. Anorg. Allg. Chem. **1988**, 560, 65.

[16] P. Mastrorilli, C. F. Nobile, F. P. Fanizzi, M. Latronico, Chunhua Hu, U. Englert, Eur. J. Inorg. Chem., **2002**, 1210.

[17] D. K. Wicht, S. N. Paisner, B. M. Lew, D. S. Glueck, G. P. A. Yap, L. M. Liable-Sands, A. L. Rheingold, C. M. Haar, S. P. Nolan, Organometallics, **1998**, 17, 652.

[18] P. Mastrorilli, Eur. J. Inorg. Chem., **2008**, 4835.

[19] W. Domańska-Babul, J. Chojnacki, E. Matern, J. Pikies, J. Organomet. Chem. **2007**, 692, 3640.

[20] W. Domańska-Babul, J. Chojnacki, E. Matern, J. Pikies, Dalton Trans. **2009,** 146.

[21] E. Baum, E. Matern, A. Robaszkiewicz, J. Pikies, Z. Anorg. Allg. Chem. **2006**, 632, 1073.

[22] I. Kovacs, H. Krautscheid, E. Matern, G. Fritz, J. Pikies, Z. Anorg. Allg. Chem. **1997**, 623 1088.

[23] G. Fritz, E. Matern, H. Krautscheid, R. Ahlrichs, J. Olkowska, J. Pikies, Z. Anorg. Allg. Chem. **1999**, 625, 1604.

[24] E. Matern, J. Olkowska-Oetzel, J. Pikies, G. Fritz, Z. Anorg. Allg. Chem., **2001**, 627, 1767.

[25] F. Basolo, Coord. Chem. Rev., **1996**, 154, 151.

[26] R. G. Pearson, Inorg. Chem., **1973**, 12, 712.

[27] H. Goesmann, E. Matern, J. Olkowska-Oetzel, J. Pikies, G. Fritz. Z. Anorg. Allg. Chem., **2001**, 627, 1181.

[28] The NMR data and X-ray structure of LiCl·2{$(Et_2N)_2P$–PLi–P^tBu_2}·2THF will be published elsewhere.

[29] B. K. Schmiedeskamp, J. G. Reising, W. Malisch, K. Hindahl, R. Schemm, W. S. Sheldrick, Organometallics, **1995**, 14, 4446.

[30] T. G. Appleton, M. A. Benett, Inorg. Chem., **1978**, 17, 738.

[31] G. M. Sheldrick, SHELX- 97. Programs for the solution and the refinement of crystal structures from diffraction data.

[32] CrysAlis RED, Oxford Diffraction Ltd., Version 1.171.29.9 (release 23-03-2006 CrysAlis171. NET) (compiled Mar 23 2006,23:39:28).

[33]]. H. Krautscheid, E. Matern, G. Fritz, J. Pikies. Z. Anorg. Allg. Chem., **2000**, 626, 253.

[34] G. Fritz, H. Goesmann, B. Mayer, Z. Anorg. Allg. Chem. **1992**, 607, 26.

[35]. A. Wisniewska, K. Baranowska, J. Pikies, Acta Cryst. **2008**, E64, m967.

[36] G. Schultz, N. Y. Subbotina, C. M. Jensen, J. A. Golen, J. Hargittai, Inorg. Chim. Acta **1992**, 191, 85.

[37] T. A. Albright, R. Hoffmann, J. C. Thibeault, D. L. Thorn, J. Am. Chem. Soc. **1979**, 101, 3801.

[38] a) S. Loss, C. Windauer, H. Grützmacher, Angew. Chem. **1999**, 111, 3546; b) Angew. Chem. Int. Ed. **1999**, 38, 3329.

[39] J. Chojnacki, A. Robaszkiewicz, E. Matern, E. Baum, J. Pikies, Acta Cryst. (2007) **E63**, m680-m683

[40] E. Matern, J. Pikies, G. Fritz, J. Pikies. Z. Anorg. Allg. Chem. **2000**, 626, 2136.

[41] I. Kovacs, H. Krautscheid, E. Matern, E. Sattler, G. Fritz, W. Hönle, H. Borrmann, H.G. von Schnering, Z. Anorg. Allg. Chem. **1996**, 622, 1564.

[42] G. Fritz, T. Vaahs, Z. Anorg. Allg. Chem. **1987**, 552, 18.

[43] I. Kovacs, E. Matern, G. Fritz, Z. Anorg. Allg. Chem. **1996**, 622, 935.

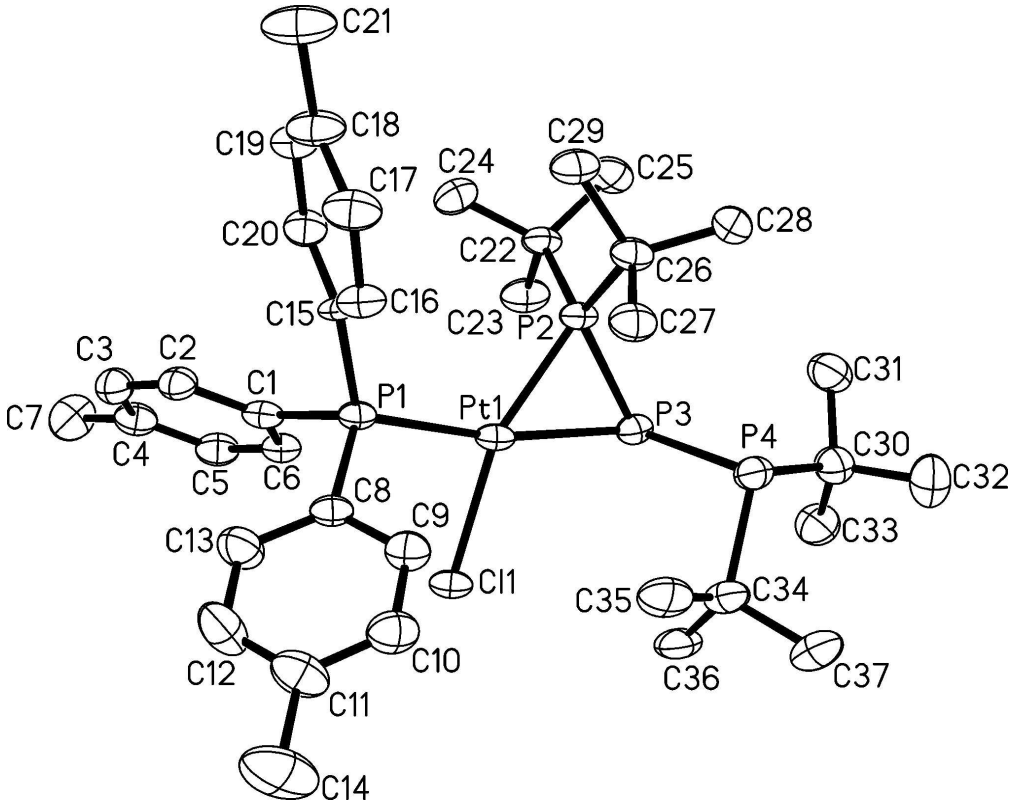

FIGURE 1. An ORTEP view of the molecular structure of 1a in the crystal; hydrogen atoms not shown, ellipsoids are drawn at 30% probability level. Selected bond lengths [pm] and angles [°]: Pt1-Cl1 236.37(15); Pt1-P1 228.53(17); Pt1-P2 221.24(16); Pt1-P3 240.77(18); P2-P3 214.50(2); P3-P4 221.80(3); P2-Pt1-P3 55.14(6); P2-P3-P4 106.92(10).
171x136mm (600 x 600 DPI)

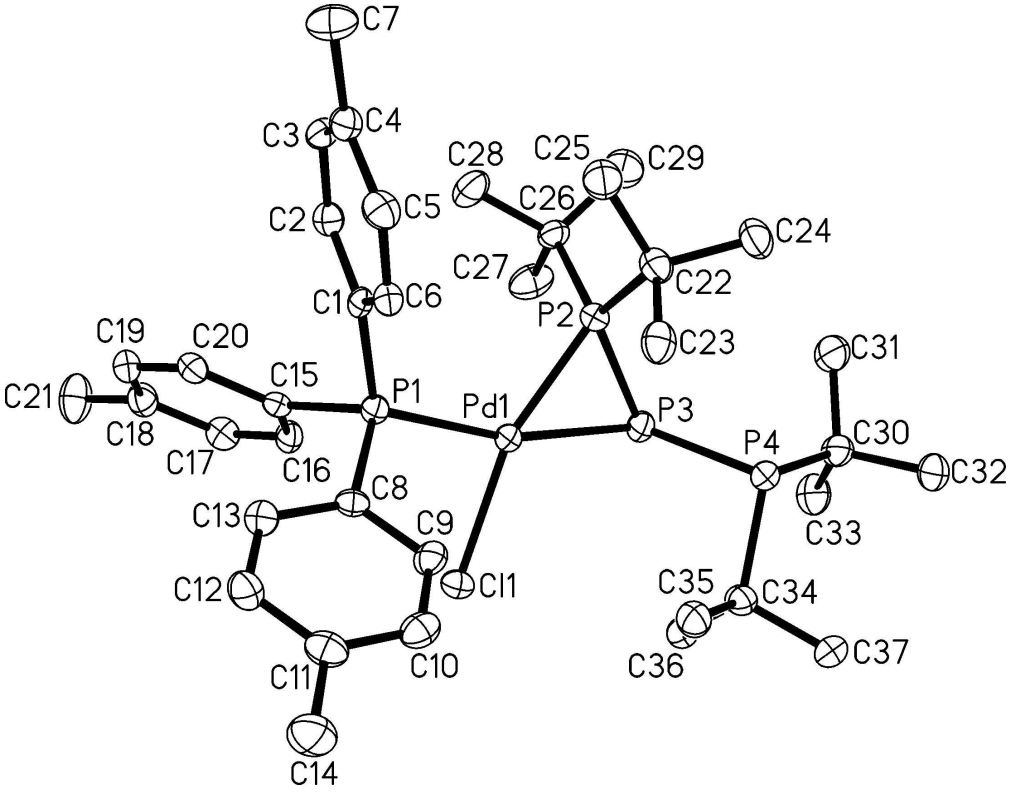

FIGURE 2. An ORTEP view of the molecular structure of 2a in the crystal; hydrogen atoms not shown, ellipsoids are drawn at 30% probability level. Selected bond lengths [pm] and angles [°]: Pd1-Cl1 238.62(9); Pd1-P1 234.32(9); Pd1-P2 223.15(9); Pd1-P3 241.79(9); P2-P3 213.03(13); P3-P4 222.40(13); P2-Pd1-P3 67.28(4); P2-P3-P4 106.78(5).
187x145mm (600 x 600 DPI)

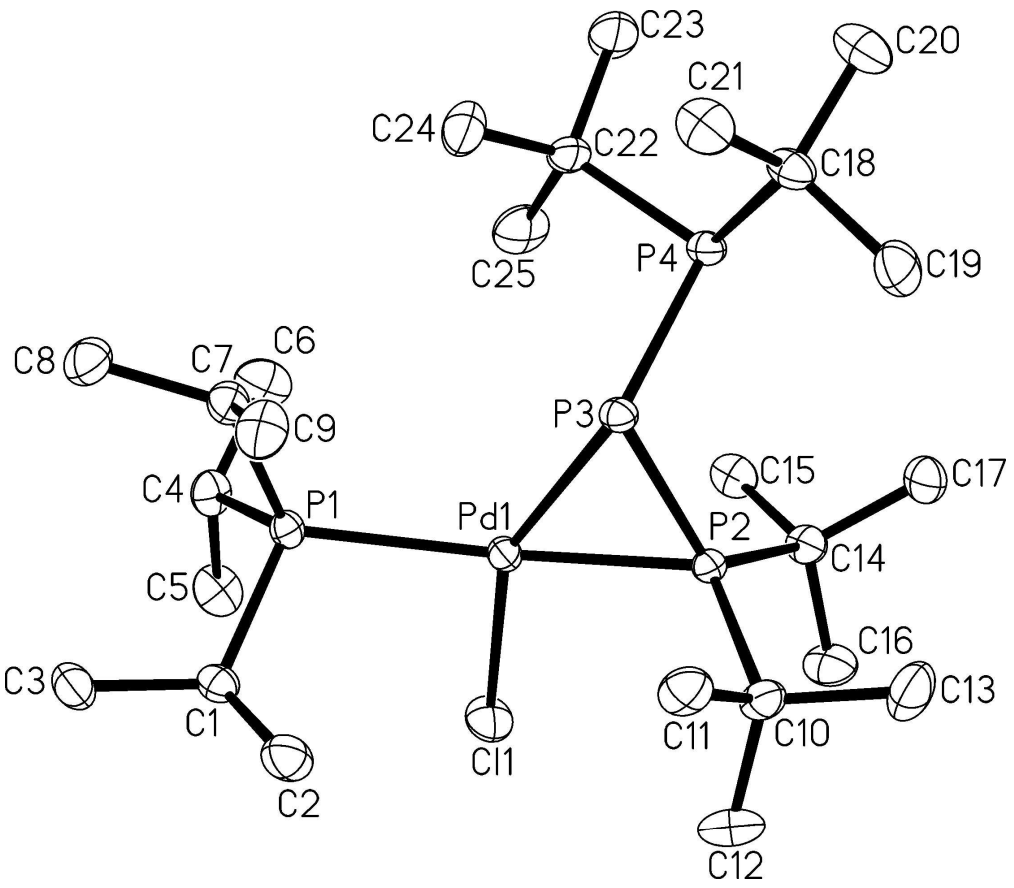

FIGURE 3. An ORTEP view of the molecular structure of 3b in the crystal; hydrogen atoms not shown, ellipsoids are drawn at 30% probability level. Selected bond lengths [pm] and angles [°]: Pd1-Cl1 237.63(5); Pd1-P1 238.77(5); Pd1-P2 225.39(5); Pd1-P3 238.59(5); P2-P3 213.32(7); P3-P4 224.05(7); P2-Pd1-P3 54.654(17); P2-P3-P4 102.96(3).
189x164mm (600 x 600 DPI)

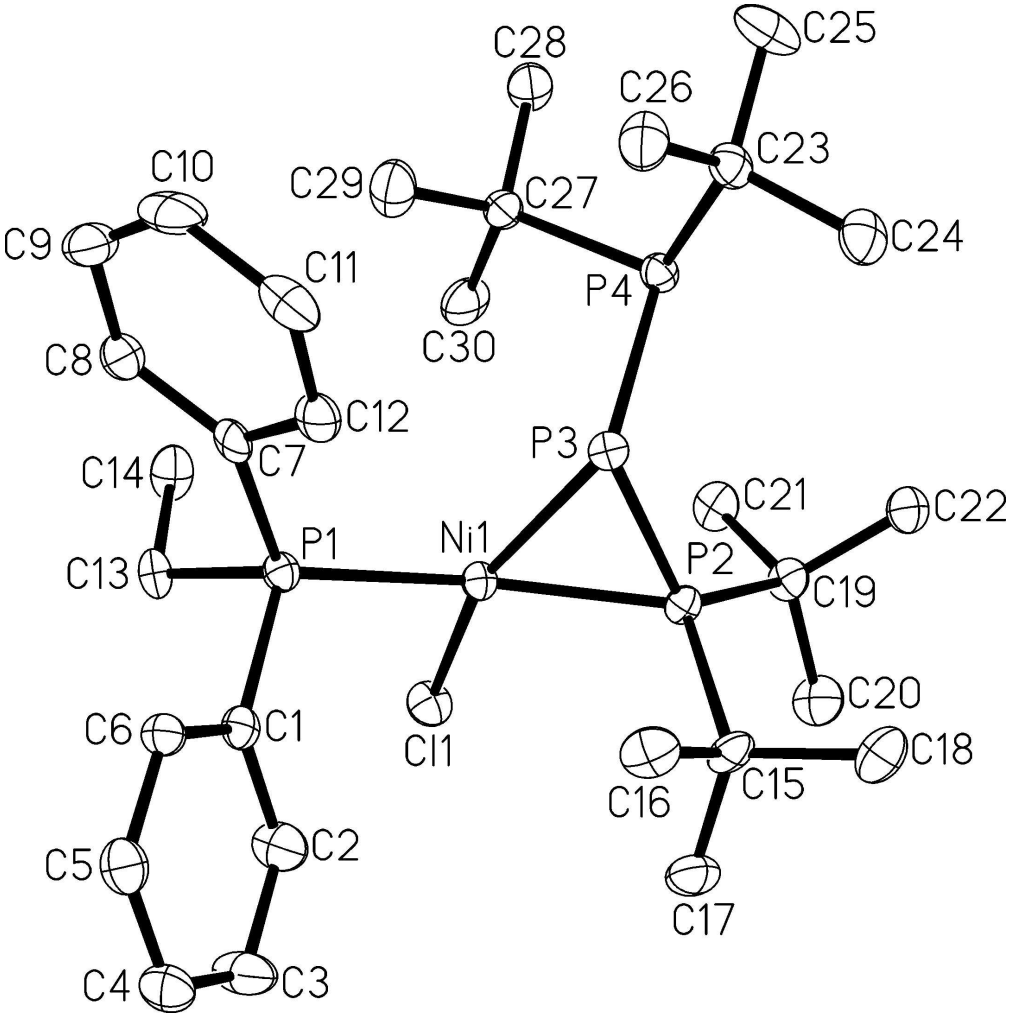

FIGURE 4. An ORTEP view of the molecular structure of 4b in the crystal; hydrogen atoms not shown, ellipsoids are drawn at 30% probability level. Selected bond lengths [pm] and angles [°]: Ni1-Cl1 220.46(9); Ni1-P1 223.68(10); Ni1-P2 214.83(10); Ni1-P3 226.05(10); P2-P3 212.54(12); P3-P4 224.80(12); P2-Ni1-P3 57.58(3); P2-P3-P4 105.58(5).
182x184mm (600 x 600 DPI)